

Thermodynamic Performance Modelling of Solar Brayton Cycle (SBC) and Integrated Solar-Thermal Brayton Cycle (ISBC) using the GE LM 6000PA Gas Turbine

¹Stephen Ejouwokoghene Henry, ²Wunuken Carlos Solomaon, ²Samuel Mary, ³Bonet Mathias Usman, ⁴Isiaka Isah, ⁵Agbogou Obinna Emmnuel, ⁶Nurudeen Mohammed Lawal

¹Department of Maintenance-Mechanical, Anoh Gas Processing Company (AGPC), Assa, Imo State, Nigeria

²Department of Mechanical Engineering, Nigeria Defence Academy (NDA), Kaduna State, Nigeria

³Department of Aerospace Engineering, Air Force Training Institute (AFIT), Kaduna State, Nigeria

⁴Centre for Atmospheric Research (CAR)-National Space Research and Development Agency (NASRDA), Prince Abubakar Audu University Campus Anyigba Kogi State, Nigeria

⁵Department of Research and Development, Defence Industries Corporation of Nigeria (DICON), Kaduna State, Nigeria

⁶Department of Science and Technology Education, Bayero University Kano State, Nigeria

Date of Submission: 01-05-2026

Date of Acceptance: 09-05-2026

Abstract

Nigeria's persistent power generation deficit, despite abundant energy resources, necessitates sustainable alternatives to conventional gas turbine plants. This study performed thermodynamic performance modelling of the Solar Brayton Cycle (SBC) and Integrated Solar-Thermal Brayton Cycle (ISBC) using the GE LM 6000PA gas turbine as the prime mover under Northern Nigerian climatic conditions. Meteorological data for Kaduna State spanning 30 years (1991–2020) were obtained from Nigeria Meteorological Agency (NiMet) and used to simulate turbine performance with Aspen HYSYS V11, both with and without solar heating. Results show that ambient temperature significantly affects conventional gas turbine output, with shaft power decreasing as ambient temperature increases. Integration of solar heating reversed this trend, raising average shaft power from 25.58 MW without solar to 40.77 MW with solar at maximum temperature, and from 25.35 MW to 41.62 MW at minimum temperature. This represents a 60–65% improvement in power output due to solar-assisted air preheating, which reduces fuel consumption required to achieve desired turbine inlet temperature. Validation against the Mercury 50 solar turbine confirmed consistency in performance trends and thermodynamic behaviour. The ISBC configuration demonstrates strong potential for improving power output, fuel savings, and emission reduction in Nigeria. Findings support deployment of ISBC systems in high-irradiation regions like Northern Nigeria to enhance grid stability and energy sustainability.

Keywords: Solar Brayton Cycle, Integrated Solar-Thermal Brayton Cycle, GE LM 6000PA, Gas Turbine, Aspen HYSYS V11, Thermodynamic Modelling, Solar Integration, Power Generation

I. Introduction

Electricity has become a key feature in Nigerian after it was discovered in the later part of the 19th century. From then on, demand began to surge due to increased urbanization and industrialization. However, generation has not kept pace despite abundant energy resources. Power supply remains poor and inadequate. The country is grappling to sustain a daily average generation of 3800 MW. Generated power fluctuates between 3000 to 5000 MW. As of 0600 hrs on Thursday, 11th July, 2019, total power generated was 3627 MW of the total installed capacity of 12910.40 MW out of which 7652.60 MW was the capacity for a transmission wheeling output of 8100 MW. The peak ever generated was 5375 MW in 2001, while in 2022 alone, the power grid collapsed twice in one week [1][2][3][4].

When contrasted with a population of over 200 million, this translates to a very low kilowatt-hour (kWh) per capita consumption, a measure of the people's material well-being. The Central Intelligence Agency (CIA) fact book puts the kWh per capita for Nigeria at 129 kWh as against 304.62 for about 30 million people and 3787.27 for 57 million populations for Ghana and South Africa respectively. This deficit persists despite huge investments. As of July 15th 2019, the President of the country then, Late President Muhammad Buhari

said “The present administration has invested Nine Hundred Billion Naira (N900B) in the power sector since assumption in office 2020” [5][4].

Stable and sustainable power supply is key to urbanization and industrial development. However, its lack constitutes a major hindrance to the growth of the Nigerian economy. Besides, environmental pollution from installed gas turbines, decreasing fossil fuel reserves, legislative pressure, and erratic fuel supply are some of the factors that have necessitated the search for alternatives to complement or possibly replace existing plants in Nigeria [2][3].

Consequently, there is a dire need to expand the megawatt generated sustainably to meet increasing demand. One viable pathway is the integration of renewable energy sources into the country’s energy mix. Among these, the Solar Brayton Cycle (SBC) and Integrated Solar-Thermal Brayton Cycle (ISBC) present promising options due to their compatibility with existing gas turbine infrastructure. This study therefore performs thermodynamic performance modelling of SBC and ISBC configurations using the GE LM 6000PA gas turbine as the prime mover. The GE LM 6000PA, widely deployed in Nigeria, offers operational flexibility and high efficiency, making it suitable for solar integration studies. The aim is to evaluate performance parameters, fuel savings, and emission reduction potential under Nigerian solar conditions, thereby providing data to mitigate the challenge of inadequate and unsustainable power generation. The current paper discusses thermodynamic modelling of the Solar Brayton Cycle (SBC) and Integrated Solar-Thermal Brayton Cycle (ISBC).

Several studies have been carried out by various researchers. In 2010, the first documented attempt to hybridize the solar gas turbine was carried out by the Solar Hybrid Gas Turbine Electric (SOLGATE) power system in Plataforma Solar de Almería, Spain. This initial design was basically the development of a SHGT equipped to directly heat pressurized air. The gas turbine was later on modified for external air heating. The investigation carried out in this work was to develop a system capable of moving the temperature of air from ambient to 1000°C. Results and expected performance were found satisfactory [6]. The European Commission reported the results of a Solar Hybrid Power and Cogeneration (SOLHYCO) plant project conducted in 2011 to develop a 100KW prototype for cogeneration based on a standard commercial micro-turbine. Different configurations of the systems and combined cycle systems were used to predict the performance and cost of the generated electricity. A key conclusion from the study revealed a viable

economic implication but low energy conversion efficiency [7]. Andrew et al [8] attempted solar electricity production by integrating a two-step air-brayton cycle for heat storage based on redox reactions. The two steps of the heat storage cycle are encompassed by a high-temperature thermolysis of Ca_3O_4 to CaO and O_2 under vacuum pressure utilizing concentrated solar radiation for process heat; and (2) the highly exothermic re-oxidation of CaO with O_2 at elevated pressures, resulting in Ca_3O_4 and providing the heat input to the air cycle. A maximum cycle efficiency of 44% was determined for re-oxidizing the CaO at 30 bar, with the maximum cycle efficiency reducing to 26% for a decrease in pressure to 5 bar. In the case of the Combined Cycle Gas Turbine, CCGT, for example, Amelio et al. [9] proposed to heat up the combustion air by passing it through PTCs, managing without an intermediary HTF. Thus, the pressurized air coming out of the compressor is sent to the solar field where is preheated up to 580°C, prior to enter the combustion chamber. The authors estimated a fossil fuel saving of 22% at design conditions, and 15.5% evaluating the annual performance. Alfonso et al. [10] proposed a configuration that integrates solar contribution to preheat the combustion air, but with the peculiar feature of a prior use of the air exiting the compressor to preheat water, that is then incorporated to the heat recovery steam generator, HRSG. Although the air is thus previously cooled, the desired TIT is achieved, and the solar contribution is finally higher, which results in a greater power generation and fossil fuel saving. Other designs by Rovira et al. [11] also proposed the use of a CR, to preheat the combustion air, compare the annual performance of a reference CCGT with the performance of two ISCC layouts that differ in the solar heat integration option which are the conventional ISCC scheme and the second scheme in which the solar heat is used to preheat the Brayton cycle combustion air. The results obtained show that ISCC with combustion air preheating suffered a reduction in yearly energy production in comparison to the reference CCTG, as a consequence of the pressure drop in the solar heat exchanger. The end goal of the project by Huseyin et al. [13] was to produce electricity at the cost of 0.06 US \$/kWh and/or lower. A Connection to local and national grids with minimum carbon emissions was also proposed. After incorporating this proposal into prevailing market situations, considering lower or zero interest rates, the values of levelized cost of energy, LCOE, and mean levelized cost of energy, MLCOE, were discovered to be lower and the payback period shorter. The open and direct solar thermal Brayton cycle with a solar dish diameter of 5.2 m and an off-the-shelf microturbine, should be

able to operate optimally in various solar beam irradiance and wind speed scenarios [13], and results showed that the optimum operating point decreases as the wind speed increases. The paper by Prosin T. et al. [16] presents initial modelling results of a centrifugal receiver (CentRec) system, using hourly weather data of regional Australia for a 100kWe microturbine as well as a more efficient and cost effective 4.6MWe unit. The optimized design for 15 hours of thermal storage capacity resulted in a tower height of 35m and a solar field size of 2100m² for the 100kWe turbine, plus a tower height of 115m and solar field size of 50 000m² for the 4.6MWe turbine. The TIT of both systems were documented at 1150°C which is greater than what the conventional microturbine systems can provide. System evaluations of the two particle receiver systems, with a selection of cost assumptions, were then compared to the current conventional means of supplying energy in such remote locations. A thermodynamic model for a hybrid solar gas-turbine power plant was presented by Camerretti et al [17]. The system consists of a micro gas turbine (100 - 110 kW) supported by a solar field to integrate heat for the regeneration and combustion through heat exchangers. In this way, a hybrid thermal energy supply was considered, combining the use of biogas with thermal power from a solar field. The overall plant performance was estimated by the Thermoflex software, a modular program that allows assembling a model with several components. In a second phase, the authors also carried out a CFD analysis of the reacting flow through the micro GT combustor when supplied with a typical biogas from anaerobic digestion in replacement of the conventional natural gas, in order to check the combustion effectiveness and the environmental impact of the gas turbine at several load levels and ambient conditions. The CFD modeling was performed by using the Fluent flow solver. The impact of the optical properties on the annual performance of flat plate collectors in a Swedish climate has been estimated by Bengt H. et al [18]. The collector parameters were determined with a theoretically based calculation program, verified from laboratory measurements. The importance of changes in solar absorptance and thermal emittance of the absorber, the addition of a Teflon film or a

Teflon honeycomb, antireflection treatment of the cover glazing, and combinations of these improvements were investigated. The results show that a combined increase in absorptance from 0.95 to 0.97 and a decrease in emittance from 0.10 to 0.05. The increase in performance by installing a teflon film as second glazing was estimated to 6% at 50°C and 14% at 70°C. If instead, a Teflon honeycomb were to be installed, a twice as high-performance increase would be obtained, 12% and 27% respectively [18]. Antireflection treatment of the cover glazing increases the annual output by 6% and 8% at 50° and 70°C, respectively. A combination of absorber improvements together with a Teflon honeycomb and an antireflection-treated glazing results in a total increase of 25% and 45% at these temperatures. The impact of using a structured cover glazing as well as external booster reflectors was also investigated. Thermodynamic modelling of SBC and ISBC is considered in this current work.

II. Methodology

This study explores the performance of thermodynamic modelling of a Solar Brayton Cycle (SBC) and Integrated Solar-Thermal Brayton Cycle (ISBC) for electric power generation in Northern Nigeria using the GE LM 6000PA gas turbine as a baseline model. Integrated Solar-Thermal Brayton Cycle (ISBC) technology as a sustainable and decentralized alternative to conventional simple Brayton cycle (SBC) systems were explored.

Kaduna State was used as a study location because it is characterized by high solar irradiation. The study period covered 30 years spanning from 1985-2020 and the meteorological data covering the period was obtained from the Nigerian Meteorological Agency (NiMet). The data values have been grouped into decades for better presentation and a 30-year average value obtained to be used for further analysis of the proposed ISBC as shown table 4.1. The study procedure utilized modelling and simulation using Aspen HYSYS V11.

The spatial distribution of the average daily solar irradiation for Kaduna State, Nigeria is shown in Figure 3.1 with its values expressed in kWh/m²/day [19].

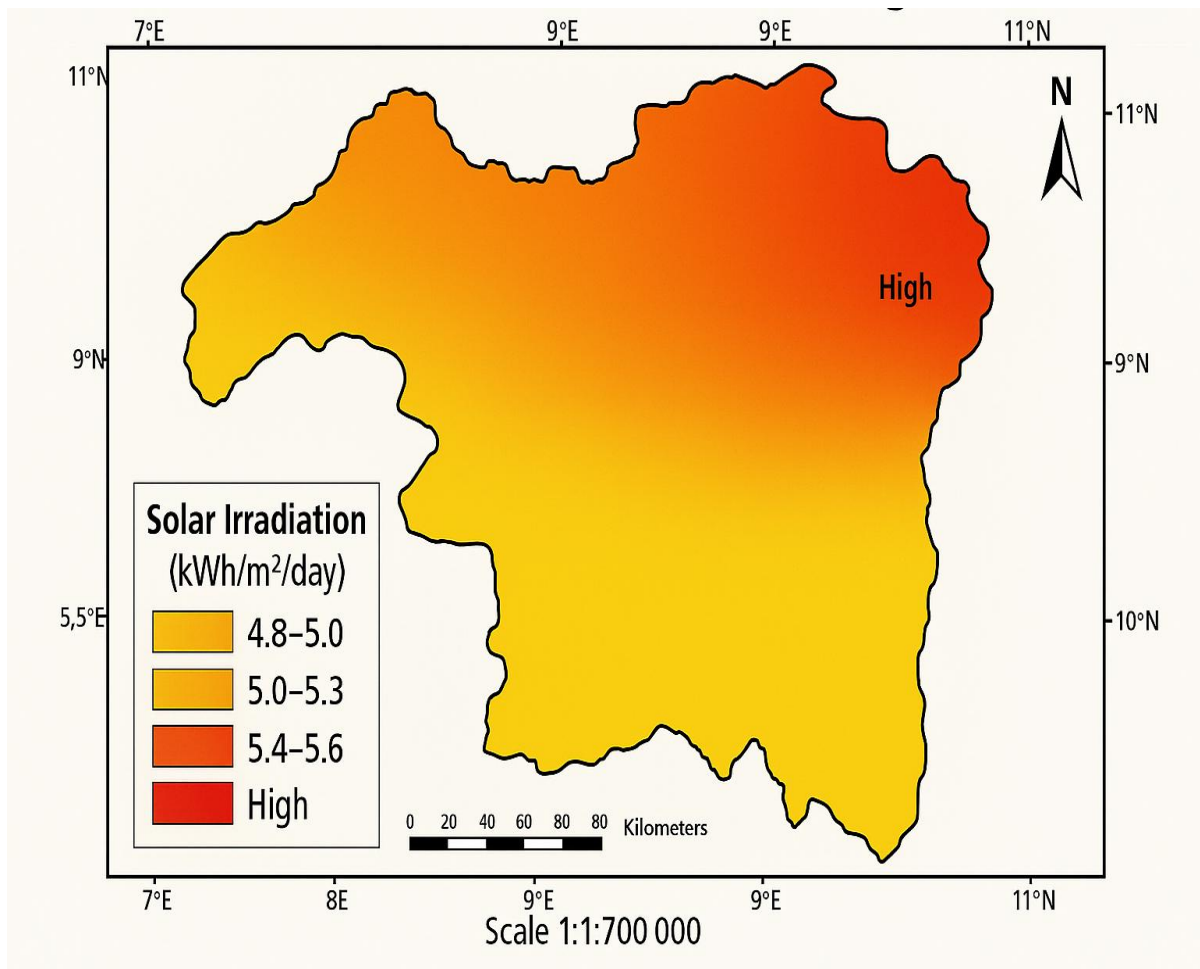


Figure 3.1: Spatial distribution of the average solar irradiation for Kaduna State, Nigeria

2.1 Modelling of the SBC and ISBC

In order to carry out performance analysis, it is necessary to first model the SBC and ISBC, and the modelling was done with Aspen HYSYS V11.

2.1.1 Optical Modelling of the SBC

The schematic diagram of the gas turbine set up with solar heater is presented using plate 3, as provided by Aspen. Each component and stream are labelled accordingly. The blue stream represents the material stream while the red stream represents the energy stream.

2.3 Determination of Performance Characteristics

The determination of the performance characteristics of the gas turbine was carried out using Aspen HYSYS V11.

2.3.1 Performance Characteristics with Aspen HYSYS 11

In order to carry out this analysis successfully, the following procedure was adopted. That is from the start up window to simulation flowsheet case environment

- i. The Aspen HYSYS V11 software was opened by double clicking on it.

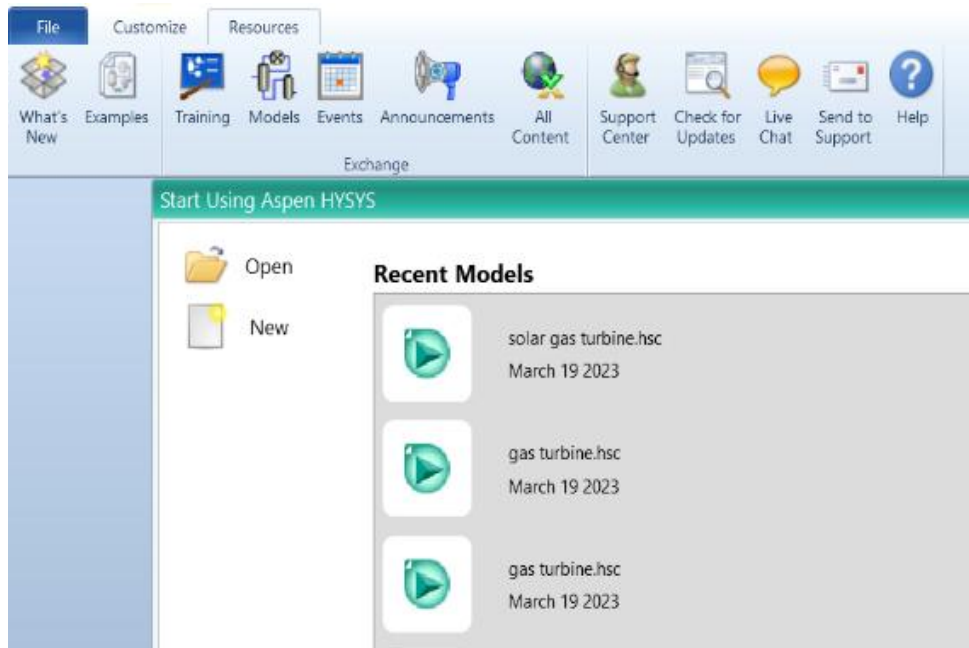


Plate 1: Aspen HYSYS V11 Start up Window

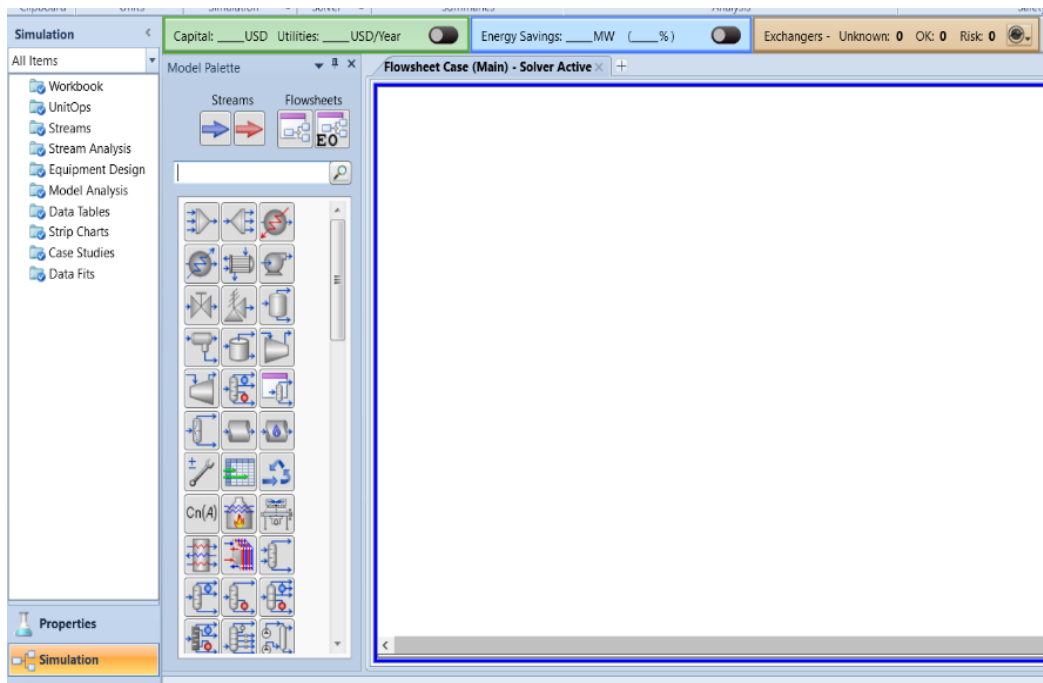


Plate 2: The Simulation Flowsheet Case Environment

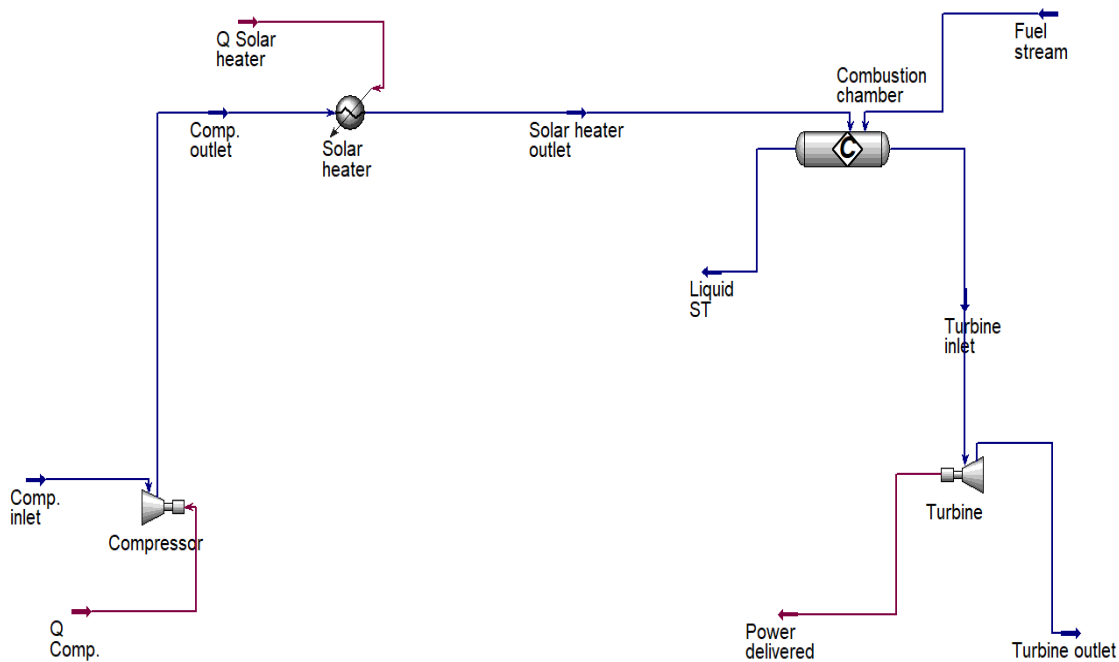


Plate 3: The Gas Turbine Model with Solar Heater

From Plate 3, Comp. inlet represent the material stream in which air flows through into the compressor. Comp. outlet represent the material stream in which compressed air flows through to the solar heater. This stream serves as the outlet of the compressor and inlet of the solar heater. Solar heater outlet represents the material stream for high pressured hot air which flows into the combustion chamber. The fuel flows through the fuel stream into the combustion chamber which is then mixed with high pressure air and burned to further heat up the air. The Liquid ST represent the material stream for the exhaust of the combustion chamber, were all the products of combustion flows through. The Turbine inlet is the stream in which the pressurised hot air flows through from the combustion chamber into the turbine, which then expand to do work. The Turbine outlet is the stream which the low pressure expanded air flows through to the atmosphere. Q Comp. is the energy stream through which the quantity of energy required by the compressor flows through into the compressor. Q Solar heater is the energy stream through which the quantity of energy required by the solar heater to raise the temperature of the pressurised air flows through. Power delivered is the energy stream through which energy required by the generator is delivered by the turbine.

The mathematical model of the energy flow across the gas turbine involves key components such as the solar collector, heat exchangers, and the gas turbine itself. This model is presented below:

- i. **Solar Collector:** this collects energy from the sun and adds the energy to the compressed air. The energy flow across the solar collector is presented below:

$$Q_{in,sc} = \eta_{sc} \times \text{Solar Irradiance} \times \text{Collector Area} \quad (1)$$

Where; $Q_{in,sc}$ = solar energy input to the collector, η_{sc} = solar collector efficiency

$$Q_{out,sc} = m \times c_p \times (T_{outlet,sc} - T_{inlet,sc}) \quad (2)$$

Where; $Q_{out,sc}$ = heat transfer to the fluid, m = mass flowrate, c_p = specific heat at constant pressure $T_{outlet,sc}$ = Outlet temperature of the working fluid from the collector, $T_{inlet,sc}$ = Inlet temperature of the working fluid to the collector

- ii. **Combustion Chamber:** this is the chamber where further energy is added to compressed air by burning it with fuel. The energy flow across the combustion chamber is presented below:

$$Q_{cc} = m \times c_p \times (T_{outlet,cc} - T_{inlet,cc}) \quad (3)$$

Where; Q_{cc} = heat added in the combustion chamber, $T_{outlet,cc}$ = Outlet temperature of the working fluid from the chambers, $T_{inlet,cc}$ = Inlet temperature of the working fluid to the chambers

- iii. **Turbine:** this is the section whereby hot combustion gas expand thereby spinning the

rotating blades. The energy flow across the turbine is presented below:

$$Q_{in,t} = m \times c_p \times (T_{inlet,t} - T_{outlet,cc}) \quad (4)$$

Where; $Q_{in,t}$ = heat input to the turbine, $T_{outlet,cc}$ = Outlet temperature of the working fluid from the chambers, $T_{inlet,t}$ = Inlet temperature of the working fluid to the turbine

$$Q_{out,t} = m \times c_p \times (T_{outlet,t} - T_{inlet,t})$$

(5)

Where; Q_{cc} = heat rejected from the turbine, $T_{outlet,t}$ = Outlet temperature of the working fluid from the turbine, $T_{inlet,t}$ = Inlet temperature of the working fluid to the turbine

The mathematical model of the work and energy flow across the gas turbine is presented below:

i. Compressor: the compressor work can be modelled using the polytropic process equation

$$W_c = c_p \times T_2 \left[\left(\frac{P_c}{P_2} \right)^{\frac{\gamma-1}{\gamma}} - 1 \right]$$

(6)

Where; W_c = compressor work, c_p = specific heat at constant pressure, T_2 = temperature of inlet fluid to the compressor, P_c = compressor pressure, P_2 = pressure of inlet fluid, γ = adiabatic index

The compressed air temperature is given by the polytropic process:

$$T_3 = T_2 \times \left(\frac{P_3}{P_2} \right)^{\frac{\gamma-1}{\gamma}} \quad (7)$$

Where; T_3 = temperature of outlet fluid from the compressor

ii. Combustion chamber: the process adds heat to the compressed air

$$Q_{cc} = c_p (T_4 - T_{31}) \quad (8)$$

Where; Q_{cc} = heat added to the combustion chamber, T_{31} = temperature of outlet to the combustion chamber.

The combustion outlet temperature depends on the efficiency of the combustion process.

iii. Turbine: the turbine work can be modelled using the polytropic process equation:

$$W_t = c_p \times T_5 \left[1 - \left(\frac{P_6}{P_5} \right)^{\frac{\gamma-1}{\gamma}} \right] \quad (9)$$

Where; W_t = turbine work, P_6 = turbine outlet pressure, P_5 = turbine inlet pressure

The turbine outlet temperature is given by the polytropic process:

$$T_6 = T_5 \left[1 - \left(\frac{P_6}{P_5} \right)^{\frac{\gamma-1}{\gamma}} \right] \quad (10)$$

iv. Network output: the network output is the difference between the work done by the turbine and the work done on the compressor:

$$W_{net} = W_t - W_c \quad (11)$$

III. Results

Table 1: Technical Specification of GT LM 6000PA

S/No.	Description	Parameters
1	Gas turbine model	GT LM 6000PA
2	Power output	42 MW
3	Turbine inlet temperature	1138 °C
4	Exhaust temperature	609 °C
5	Pressure ratio	12
6	Inlet airflow	144 kg/s
7	Fuel	Natural gas
8	Fuel heating value	43.124 MJ/kg
9	Heat rate	11818.2 KJ/kWh
10	Compressor stages	17

Table 2: Technical Specification for Mercury 50 Solar Turbines

S/No.	Description	Parameter
1	Gas turbine model	Mercury 50 solar turbine
2	Power output	4600 kWe
3	Heat rate	9350 kJ/kWe-hr
4	Compressor stage	10
5	Compressor ratio	9.9
6	Intel airflow	17.9 kg/s
7	Fuel system	Natural gas

8	Exhaust flow	63700 kg/hr (17.69 kg/s)
9	Exhaust temperature	365 °C

The meteorological data acquired from NiMet Kaduna is presented below in Table 3 [18].

Table 3: Mean Decadal Monthly Max Temperature (°C) for Kaduna (1991 – 2020)

	1991-2000	2001-2010	2011-2020	30 YR AVG
JAN	28.93	30.32	30.81	30.02
FEB	32.23	32.60	34.65	33.16
MAR	35.66	35.77	36.27	35.90
APR	35.81	36.72	36.54	36.36
MAY	33.96	33.48	34.19	33.88
JUN	31.22	30.14	31.37	30.91
JUL	29.28	28.47	29.41	29.05
AUG	28.49	27.77	28.60	28.29
SEP	30.08	29.04	30.14	29.75
OCT	31.94	30.40	32.01	31.45
NOV	31.94	30.84	32.79	31.86
DEC	29.66	29.12	30.36	29.71

Table 4: Mean Decadal Monthly Min Temperatures (°C) for Kaduna (1991 – 2020)

	1991-2000	2001-2010	2011-2020	30 YR AVG
JAN	14.28	14.64	14.99	14.64
FEB	16.57	17.27	16.54	16.79
MAR	20.78	21.05	21.38	21.07
APR	23.05	23.63	23.15	23.28
MAY	22.69	22.63	22.79	22.70
JUN	21.39	21.30	21.49	21.39
JUL	21.04	20.83	21.09	20.99
AUG	20.64	20.55	20.74	20.64
SEP	20.25	20.58	20.66	20.50
OCT	19.45	19.73	20.51	19.90
NOV	16.18	16.33	17.21	16.57
DEC	14.51	14.16	14.67	14.45

Table 5: 30 Years Mean Temperature Distribution from NiMet

Month	Max monthly mean temperature (K)	Min monthly mean temperature (K)
January	303.17	287.79
February	306.31	289.94
March	309.05	294.22
April	309.51	296.43
May	307.03	295.85
June	304.06	294.54
July	302.20	294.14
August	301.44	293.79
September	302.90	293.65
October	304.60	293.05
November	305.01	289.72
December	302.86	287.60

Table 1: Result from Aspen HYSYS V11 with Solar Heater at Max Temp

	Shaft power delivered (MW)	Turbine Entry temperature (K)	Mass flow of fuel (kg/s)	Exhaust gas temperature (K)
January	40.89	1204	0.2778	734.7
February	40.67	1205	0.2778	735.2
March	40.48	1206	0.2778	735.7
April	40.44	1206	0.2778	735.7
May	40.62	1205	0.2778	735.3
June	40.83	1204	0.2778	734.8
July	40.96	1204	0.2778	734.5
August	41.01	1204	0.2778	734.4
September	40.91	1204	0.2778	734.6
October	40.79	1204	0.2778	734.9
November	40.76	1204	0.2778	735.0
December	40.91	1204	0.2778	734.6

Table 2: Result from Aspen HYSYS with Solar Heater at Min Temp

	Shaft power delivered (MW)	Turbine Entry temperature (K)	Mass flow of fuel (kg/s)	Exhaust gas temperature (K)
January	41.95	1200	0.2778	732.2
February	41.80	1201	0.2778	732.6
March	41.51	1202	0.2778	733.2
April	41.36	1202	0.2778	733.6
May	41.40	1202	0.2778	733.5
June	41.49	1202	0.2778	733.3
July	41.51	1202	0.2778	733.2
August	41.54	1202	0.2778	733.2
September	41.55	1202	0.2778	733.1
October	41.59	1202	0.2778	733.1
November	41.82	1201	0.2778	732.5
December	41.96	1200	0.2778	732.2

Table 3: Result from Aspen HYSYS without Solar Heater at Max Temp

	Shaft power delivered (MW)	Turbine Entry temperature (K)	Mass flow of fuel (kg/s)	Exhaust gas temperature (K)
January	25.54	764.3	0.2778	452.9
February	25.62	771.0	0.2778	457.1
March	25.68	776.9	0.2778	460.8
April	25.69	777.8	0.2778	461.4
May	25.63	772.6	0.2778	458.1
June	25.56	766.2	0.2778	454.1
July	25.52	762.3	0.2778	451.6
August	25.50	760.7	0.2778	450.6
September	25.53	763.8	0.2778	452.6
October	25.58	767.4	0.2778	454.8
November	25.59	768.3	0.2778	455.4
December	25.53	763.7	0.2778	452.5

Table 4: Result from Aspen HYSYS without Solar Heater at Min Temp

	Shaft power delivered (MW)	Turbine Entry Temperature (K)	Mass flow of fuel (kg/s)	Exhaust gas temperature (K)
January	25.13	731.7	0.2778	432.5
February	25.19	736.3	0.2778	435.3
March	25.31	745.3	0.2778	441.0

April	25.37	750.0	0.2778	443.9
May	25.35	748.8	0.2778	443.2
June	25.32	746.0	0.2778	441.4
July	25.31	745.2	0.2778	440.9
August	25.30	744.4	0.2778	440.4
September	25.29	744.1	0.2778	440.3
October	25.28	742.9	0.2778	439.5
November	26.19	764.2	0.2778	452.8
December	25.12	731.3	0.2778	432.2

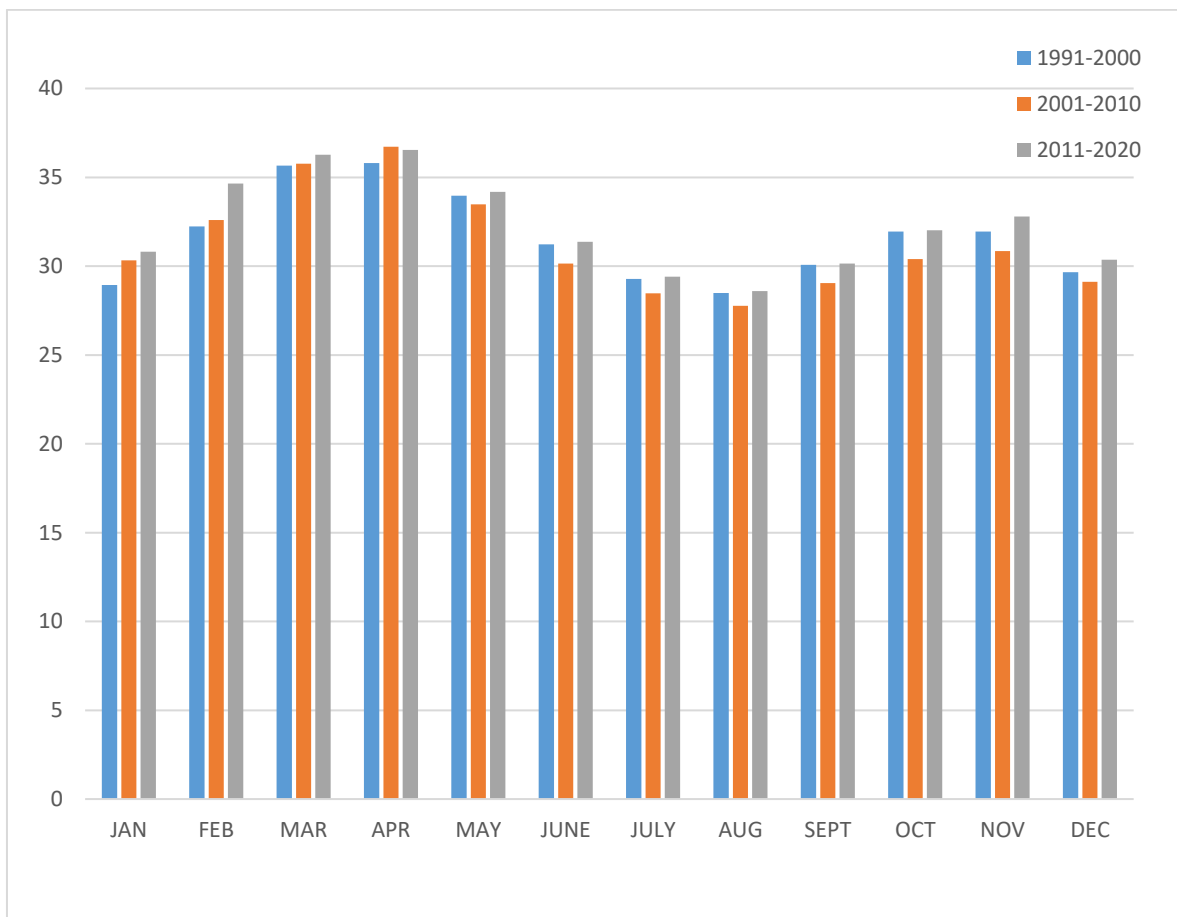


Figure 1: Mean Decadal Monthly Max Temperatures for Kaduna (1991 – 2020)

As can be seen from Table 1 and represented in Figure 1, the month of April has the highest mean maximum temperatures of 35.81°C over the period from 1991 – 2000, 36.72°C over the period from 2001 – 2010, 36.54°C over the period from 2011 – 2020 and a 30-year average of 36.36°C which is a reasonable approximate maximum temperature value for the month of April to be used for simulation and analysis. In addition to the above stated fact, the month of August, as can also be seen from Table 1

and Figure 1, presents the lowest mean maximum temperatures of 28.49°C over the period from 1991 – 2000, 27.77°C over the period from 2001 – 2010, 28.60°C over the period from 2011 – 2020 and a 30-year average of 28.29°C which is also a reasonable approximate maximum temperature value for the month of August to be used for simulation and analysis.

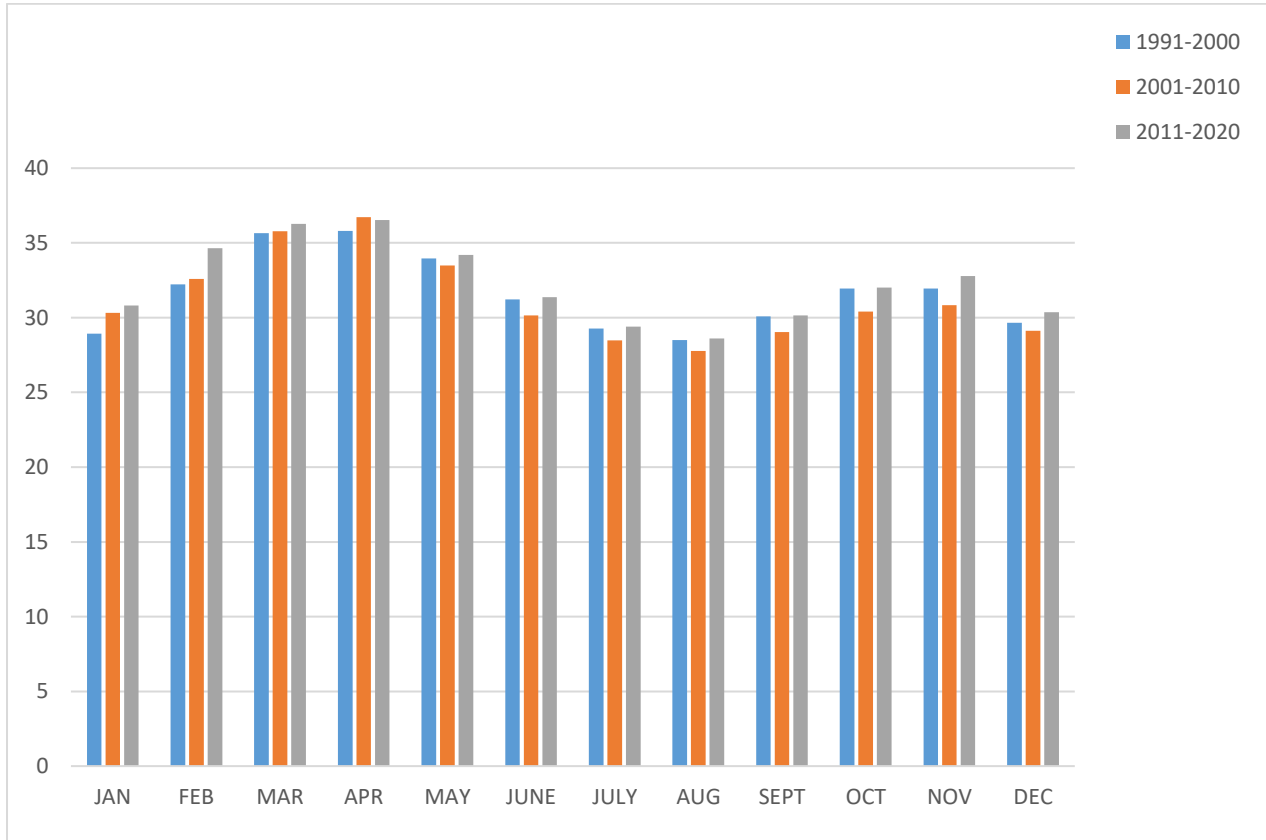


Figure 2: Mean Decadal Monthly Minimum Temperatures for Kaduna (1991 – 2020)

Interestingly, the month of August, as can also be seen from Table 2 and Figure 2, does not present the lowest mean minimum temperatures. Rather, this was earlier claimed by the month of January with an average of 14.28°C over the period from 1991 – 2000. In recent times, the month of December now claims the title of the lowest minimum temperature with values of 14.16°C over the period from 2001 – 2010, 14.67°C over the period from 2011 – 2020 and a 30-year lowest average of 14.45°C.

3.1 Results for Determination of Performance Characteristics

3.1.1 30-Year Mean Temperature Distribution (Maximum and Minimum)

The 30 years mean temperature distribution acquired from NiMet is presented in Table 4.3 below in Kelvin. This unit will serve as the temperature for the

input stream to the compressor for the performance analysis with Aspen HYSYS V11.

3.2 Simulation Results from Aspen HYSYS V11 with Solar Heater

Tables 6 and 7 give the summary of the result obtained with Aspen HYSYS V11 to simulate the performance of the GT 2020. This simulation result considers the effect of solar heating on the overall performance of the gas turbine. The simulation result is presented for both maximum and minimum temperature from January to December. Parameters such as shaft power delivered, turbine entry temperature, mass flow of fuel and exhaust gas temperature are presented in the tables earlier mentioned and tables show how these parameters varies on monthly averages from January to December.

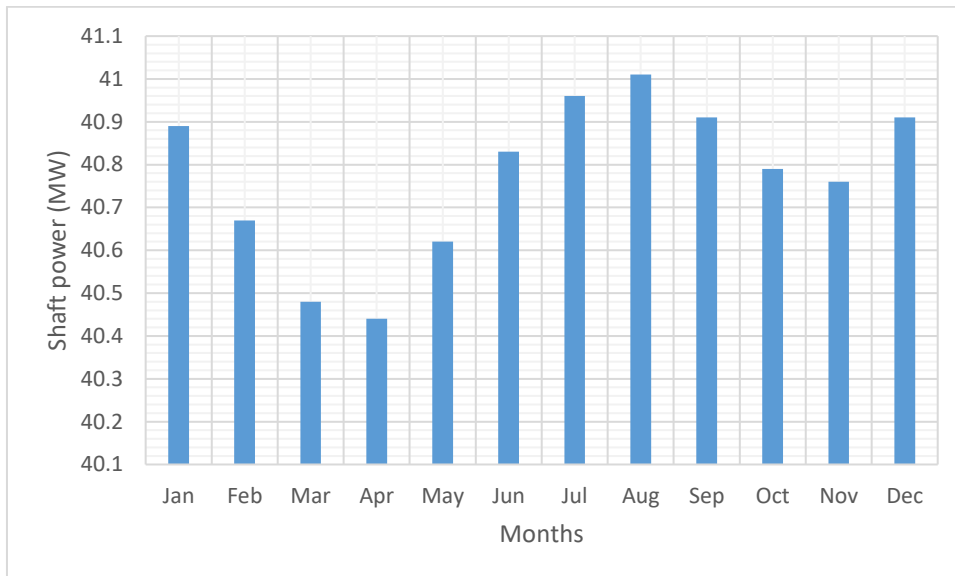


Figure 3: The Monthly Variation of Shaft Power at Maximum Temperature

The Figure 3 shows the monthly average variation of shaft power from January to December. The shaft power represents the actual mechanical power output of the gas turbine engine, and as seen from the figure, the highest mechanical power output was experienced in August with an average monthly ambient temperature of 301.44 K. while the lowest mechanical power output was experienced in April, with an average monthly ambient temperature of

309.51 K. This result shows that the gas turbine gives a higher shaft power at lower ambient temperatures and lesser shaft power at higher ambient temperature, hence regions on the graph which shows higher shaft power will correspond to regions of lower ambient temperature while regions on the graph which shows lower shaft power will correspond to higher ambient temperature.

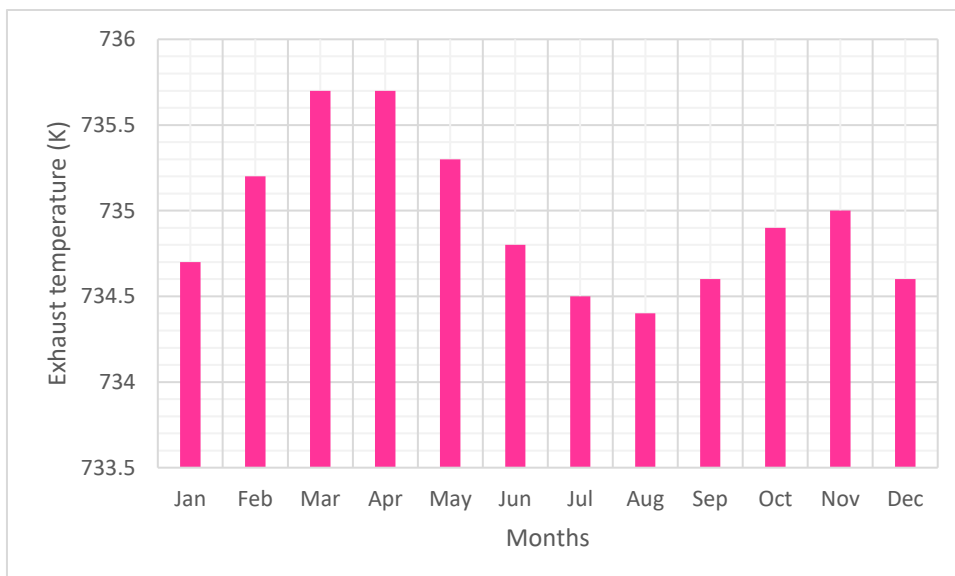


Figure 4: The Monthly Variation of EGT at Maximum Temperature

The Figure 4 shows the monthly average variation of exhaust temperature from January to December. The exhaust temperature represents the actual waste heat energy from the gas turbine engine, and as seen from

the Figure, the highest exhaust temperature was experienced in March and April with an average monthly ambient temperature of 302.86 K. while the lowest exhaust temperature was experienced in

August, with an average monthly ambient temperature of 301.44 K. This result shows that the gas turbine gives a higher exhaust temperature at

higher ambient temperatures and lesser exhaust temperature at lesser ambient temperature.

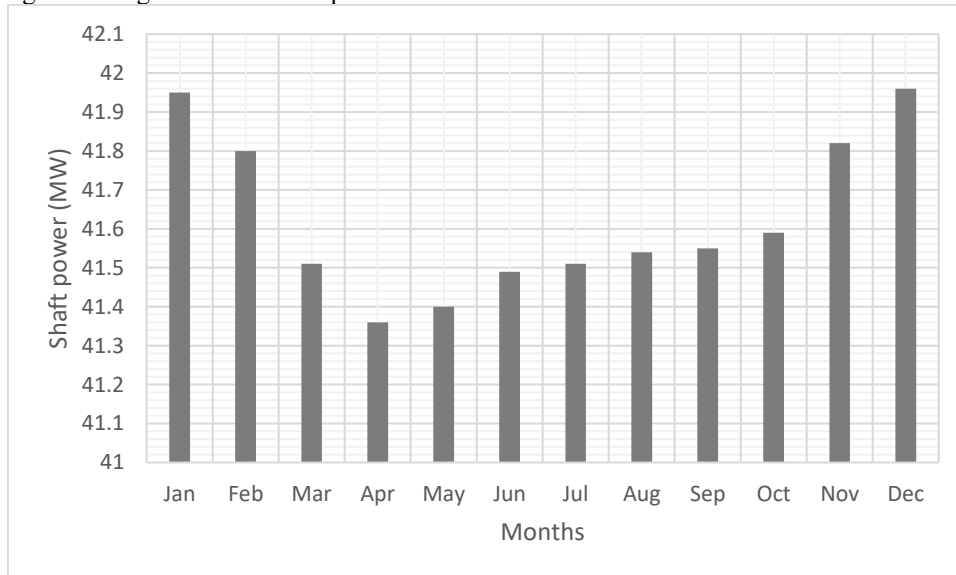


Figure 5: The Monthly Variation of Shaft Power at Minimum Temperature

The Figure 5 shows the monthly average variation of shaft power at minimum temperature from January to December. The shaft power represents the actual mechanical power output of the gas turbine engine, and as seen from the Figure, the highest mechanical power output was experienced in December with an average monthly ambient temperature of 287.60 K.

while the lowest mechanical power output was experienced in April, with an average monthly ambient temperature of 296.43 K. The trend shows that the gas turbine gives a higher shaft power at lower ambient temperatures and lesser shaft power at higher ambient temperature.

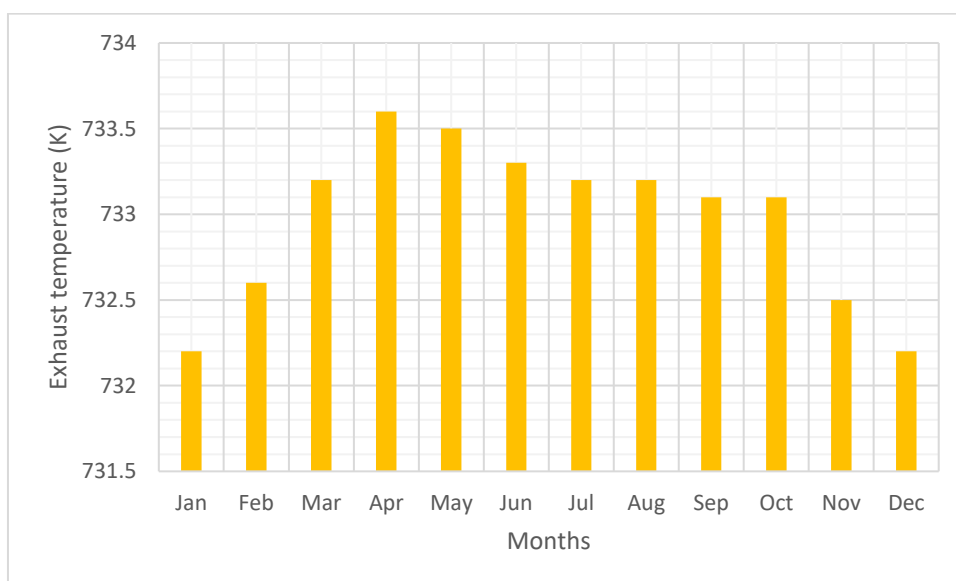


Figure 6: The Monthly Variation of EGT at Minimum Temperature

The Figure 6 shows the monthly average variation of exhaust temperature from January to December at minimum temperature. The exhaust

temperature represents the actual waste heat energy from the gas turbine engine, and as seen from the Figure, the highest exhaust temperature was

experienced in April with an ambient temperature of 296.43 K while the lowest exhaust temperature was experienced in January and December with an ambient temperature of 287.79 and 287.60 respectively. This result shows that the gas turbine gives a higher exhaust temperature at higher ambient temperature and lower exhaust temperature at lesser ambient temperatures respectively.

3.3 Simulation Results from Aspen HYSYS V11 without Solar Heater

Table 8 and 9 gives the summary of the result obtained with Aspen HYSYS V11 to simulate the

performance of the GT LM 6000PA. This simulation result does not consider the effect of solar heating on the overall performance of the gas turbine. The simulation result is presented for both maximum and minimum temperature from January to December. Parameters such as shaft power delivered, turbine entry temperature, mass flow of fuel and exhaust gas temperature are presented in those Tables. The Tables 8 and 9 show how these parameters vary on monthly averages from January to December. The summary of the values obtained for these parameters using Aspen HYSYS V11 are presented in the Tables mentioned earlier

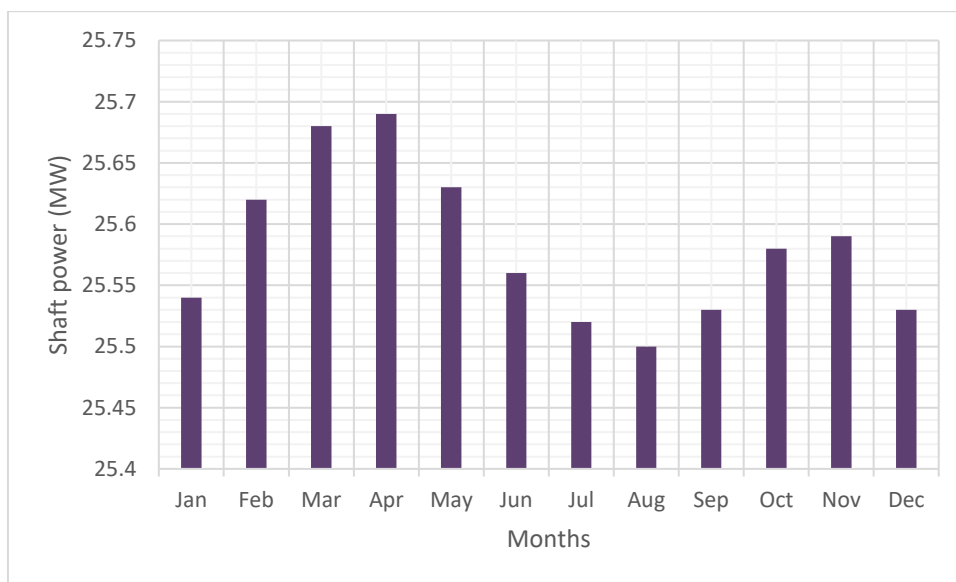


Figure 7: The Monthly Variation of Shaft Power at Maximum Temperature

The Figure 7 shows the monthly average variation of shaft power from January to December when simulation was performed without solar heating. As seen, the highest shaft power delivered was recorded in April while the lowest shaft power delivered was recorded in August. When compared with that obtained when solar heating was

considered, notable decrease in the performance was observed. This result shows that the performance of this gas turbine model will increase at higher temperature and decrease at lower temperature. The reverse will be the case when solar heating is considered.

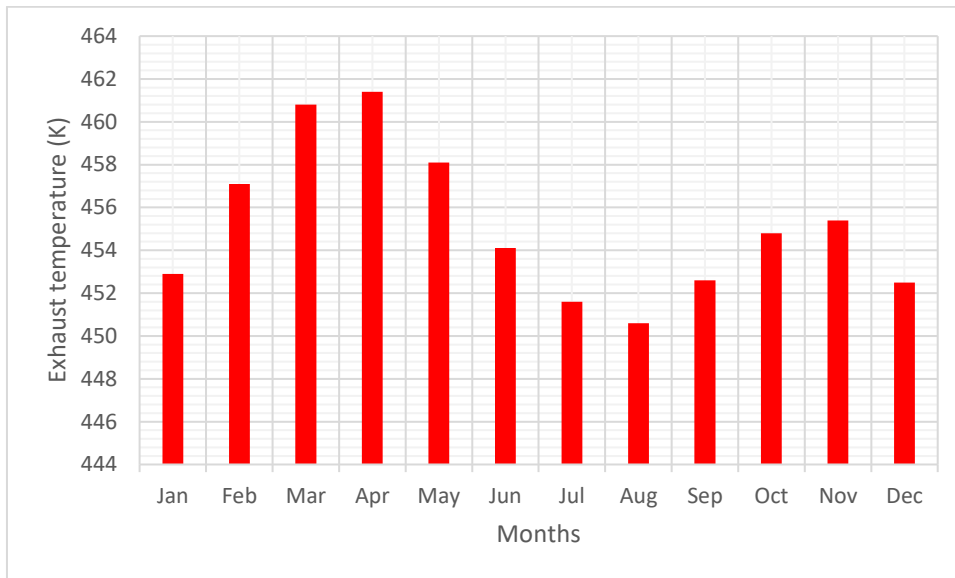


Figure 8: The Monthly Variation of EGT at Maximum Temperature

The Figure 8 shows the monthly average variation of EGT from January to December when simulation was performed without solar heating. As seen, the highest EGT was experienced in April when the ambient temperature is 309.51 K while the lowest EGT was

experienced in August when the ambient temperature was 301.44 K. The higher EGT occurred at a higher ambient temperature and lower EGT occurred at a lesser ambient temperature.

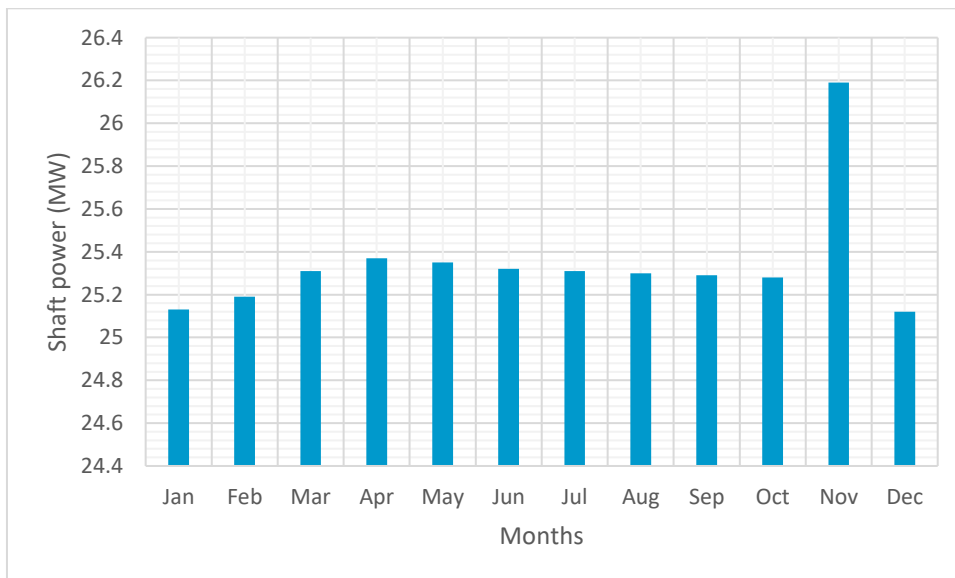


Figure 9: The Monthly Variation of Shaft Power at Minimum Temperature

The Figure 9 shows the monthly average variation of shaft power from January to December when simulation was performed without solar heating. As seen from the Figure, the highest shaft power delivered was recorded in November at an ambient temperature of 289.72 K while the lowest shaft power

delivered was experienced in December at an ambient temperature of 287.60 K. The higher shaft power occurred at higher ambient temperature while the lower shaft power occurred at lesser ambient temperature.

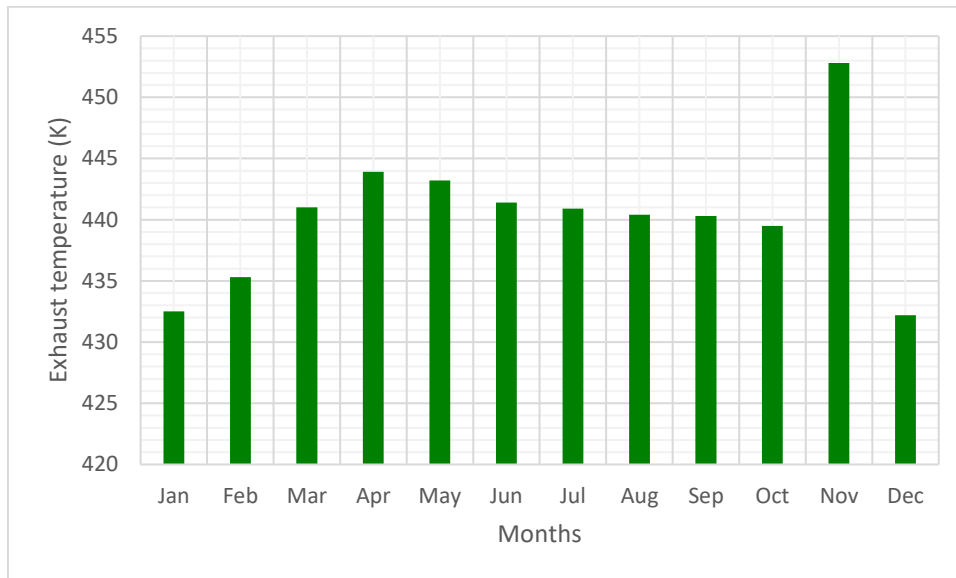


Figure 10: The Monthly Variation of EGT at Minimum Temperature

The Figure 10 shows the monthly average variation of EGT from January to December when simulation was performed without solar heating. As seen from the Figure, the highest EGT was recorded in November at an ambient temperature of 289.72 K while the lowest EGT was recorded in December at an ambient temperature of 287.60 K. The higher EGT occurred at higher ambient temperature while the lower EGT occurred at lesser ambient temperature.

3.4 Discussion of Simulation Results

3.4.1 Discussion of Simulation Results from Aspen HYSYS V11

The results presented in Tables 6 and 7 (with solar heater) and Tables 8 and 9 (without solar heater) clearly demonstrate the performance benefits of solar integration.

With the solar heater integrated, the gas turbine achieved average shaft power outputs of approximately 40.77 MW at maximum temperature and 41.62 MW at minimum temperature. The difference between these two operating conditions is

relatively small (about 2%), indicating that solar preheating of the compressed air significantly reduces the sensitivity of turbine performance to ambient temperature. The elevated turbine entry temperatures achieved through solar heat input allow higher expansion work in the turbine while maintaining a comparatively low and stable fuel mass flow rate.

In contrast, the non-solar configuration shows substantially lower performance levels. Without the solar heater, the turbine produces average shaft power outputs of only 25.58 MW at maximum temperature and 25.35 MW at minimum temperature, as shown in Tables 8 and 9. Comparing both configurations, the inclusion of the solar heater results in an increase in power output of approximately 15–16 MW, representing a 60–65% improvement over the conventional Brayton cycle. This improvement is achieved primarily through solar-assisted air preheating, which reduces the amount of fuel required to reach the desired turbine inlet temperature.

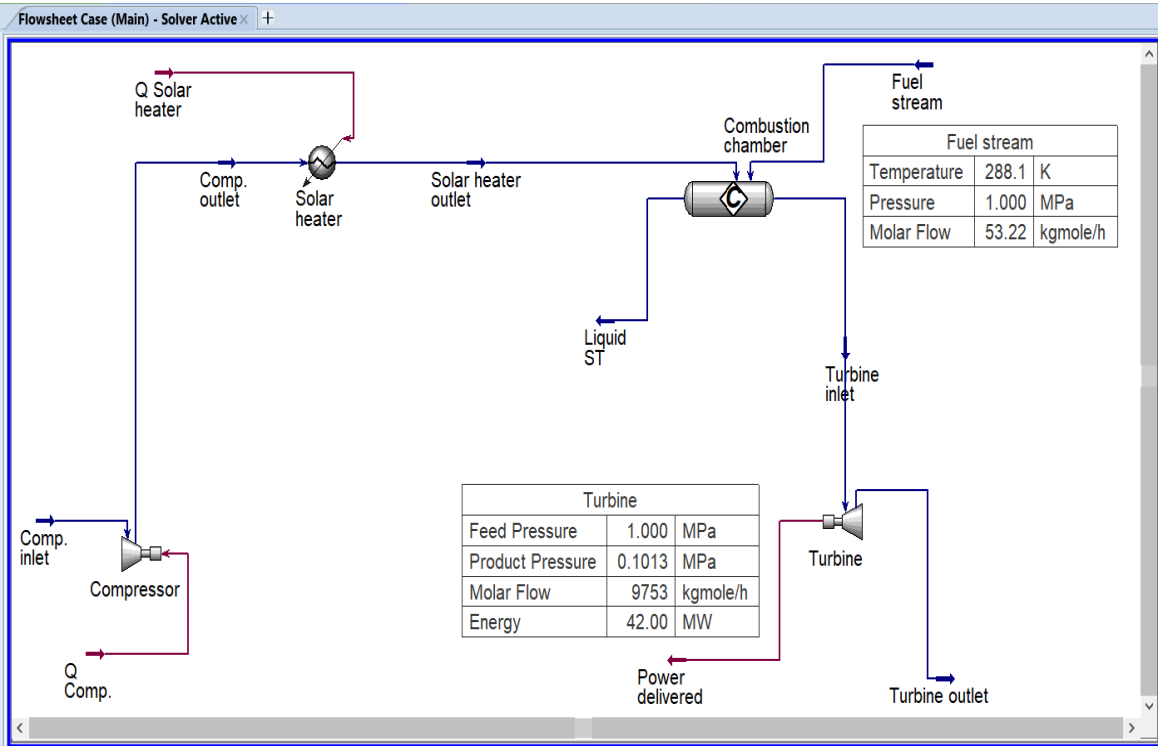


Plate 1: Simulation Flowsheet with Solar Heating at Room Temperature

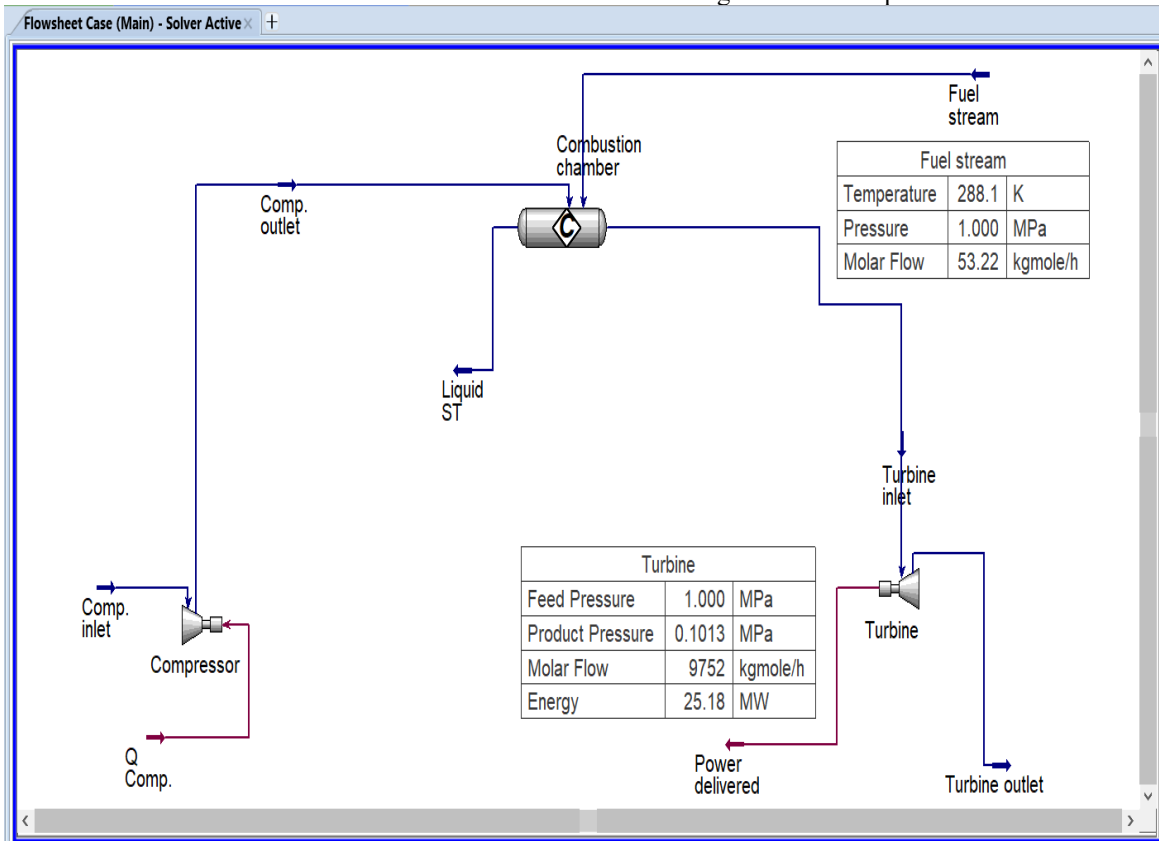


Plate 2: Simulation Flowsheet without Solar Heating at Room Temperature

3.4.2 Validation of ISBC Model Using the Mercury 50 Solar Turbine

The validity of the Integrated Solar Brayton Cycle (ISBC) model developed in this study was assessed through comparison with the Mercury 50 solar gas turbine, a commercially deployed and well-documented solar-assisted gas turbine system. The Mercury 50 was selected because it represents an operational benchmark for ISBC technology and operates on similar thermodynamic principles as the proposed model.

The technical specifications of the Mercury 50 turbine presented in Table 2 (rated power, pressure ratio, inlet airflow, exhaust temperature, and heat rate) were used as reference parameters for validation. These specifications provided realistic bounds within which the simulated results were expected to fall.

Comparative validation was achieved by examining performance trends and magnitudes rather than exact numerical equality. The simulated ISBC results obtained using Aspen HYSYS V11 and summarized in Tables 6 and 7 show turbine power output in the range of 40.77–41.62 MW, with improved thermal performance achieved through solar-assisted air preheating. Although the Mercury 50 is a smaller turbine (≈ 4.6 MW), the relative performance behaviour is consistent in both systems, particularly the enhancement of power output and efficiency due to solar thermal contribution.

Additionally, both the Mercury 50 system and the developed ISBC model exhibit similar responses to ambient temperature variations, namely improved performance at lower temperatures and moderated performance degradation at higher temperatures due to solar preheating. This agreement in behaviour confirms that the governing thermodynamic processes in the developed model accurately reflect those of an existing solar-assisted gas turbine.

Overall, the consistency between the simulated ISBC performance (Tables 6 and 7) and the known operational behaviour of the Mercury 50 solar turbine (Table 2) confirms the physical reliability and credibility of the modelling approach adopted in this work. The Mercury 50 therefore serves as an effective validation benchmark, supporting the suitability of the developed ISBC model for performance analysis under Northern Nigerian climatic conditions

IV. Conclusion

This study performed thermodynamic modelling of the Solar Brayton Cycle (SBC) and Integrated Solar-Thermal Brayton Cycle (ISBC) using the GE LM 6000PA gas turbine to evaluate

performance enhancement potential under Nigerian climatic conditions. Thirty years (30) of meteorological data for Kaduna State were used to simulate monthly performance variations with Aspen HYSYS V11.

The following conclusions are drawn from the research:

- i. Ambient Temperature Effect: Conventional gas turbine performance without solar heating is highly sensitive to ambient temperature. Shaft power output decreases with increasing ambient temperature due to reduced air density and mass flow, with lowest output recorded in hot months like April and highest in cooler months like August or December.
- ii. Solar Integration Benefit: Integration of solar heating via ISBC configuration significantly improves performance. Solar preheating of compressor discharge air raises turbine entry temperature without additional fuel, increasing shaft power by 15–16 MW. This represents a 60–65% improvement over the conventional cycle.
- iii. Reduced Temperature Sensitivity: The ISBC configuration decouples turbine performance from ambient temperature penalties. While conventional output varies widely with seasonal temperature, ISBC maintains relatively stable output year-round, with peak performance shifting to cooler months like August when both low ambient temperature and high solar irradiation coincide.
- iv. Fuel and Emission Advantage: Mass flow of fuel remained constant at 0.2778 kg/s across all solar cases, indicating that increased power output was achieved without higher fuel input. This implies substantial specific fuel consumption reduction and lower CO₂ and NO_x emissions per MWh generated.
- v. Model Validation: Performance trends of the developed ISBC model align with the operational characteristics of the Mercury 50 solar turbine, confirming the physical reliability of the Aspen HYSYS V11 model for Nigerian conditions.

The ISBC using GE LM 6000PA is technically viable for Nigeria and offers a pathway to improve generation capacity, reduce fossil fuel dependence,

and mitigate environmental impact from existing gas turbine plants.

V. Recommendations

Based on the findings of this study, the following recommendations are made:

- i. **Pilot Deployment:** The Federal Ministry of Power and private investors should initiate pilot ISBC plants in Northern Nigeria, particularly Kaduna, Kano, and Sokoto, where average daily solar irradiation exceeds 5.5 kWh/m²/day. The GE LM 6000PA provides a suitable platform due to its operational flexibility and existing footprint in Nigeria.
- ii. **Policy Support:** Government should develop incentives such as tax holidays, import duty waivers on solar field components, and feed-in tariffs for solar-gas hybrids to accelerate ISBC adoption. This aligns with Nigeria's Energy Transition Plan on research utilization for national development.
- iii. **Hybrid Dispatch Strategy:** Grid operators should revise dispatch schedules to maximize ISBC output during August–October when solar contribution and low ambient temperature coincide, thereby reducing reliance on inefficient simple-cycle operation in hot months.
- iv. **Further Research:**
 - (a) Future work should consider Techno-economic analysis to determine Levelized Cost of Energy (LCOE) and payback period for ISBC retrofits.
 - (b) Transient simulation using hourly Direct Normal irradiance (DNI) and ambient data to capture part-load and cloud-cover effects.
 - (c) Exergy analysis to identify irreversibilities in the solar receiver and heat exchangers for design optimization.
 - (d) Emission quantification of CO₂, NO_x, and SO_x reduction achievable with ISBC compared to baseline GE LM 6000PA.
- v. **Capacity Building:** Technical training on Aspen HYSYS and solar-thermal integration should be incorporated into engineering curricula to build local competence and skill acquisition.
- vi. **Data Monitoring:** NiMet and Transmission Company of Nigeria (TCN) should collaborate to establish high-resolution solar and ambient data stations at existing gas turbine sites to

enable site-specific ISBC feasibility studies.

Acknowledgment

The authors appreciate the Almighty God for milestones achieved so far.

REFERENCE

- [1] Claudius A. A., Ph.D (2020), Nigeria Electricity Industry: Issues, challenges and solutions, Public Lecture Series, College of Engineering, Covenant University, Ota, Vol. 8, No. 2, October, 2020
- [2] Energy Mix report, The *Nigerian* Electricity Regulatory Commission (NERC), March 12th, 2021
- [3] Energy Mix report, The *Nigerian* Electricity Regulatory Commission (NERC), February 28th, 2021
- [4] The Nigerian Tribune, Nigeria has to have the world's worst electricity crisis, March 19th, 2022.
- [5] The Paris Agreement on Climate change. December, 2020 [Accessed January 15, 2019]
- [6] SOLGATE, Solar hybrid gas turbine electric power system. Tech. rep. EUR 21615, European Commission; 2010, [Accessed February 10, 2019]
- [7] 6. Hybrid Optimization Model for Electrical Renewables (HOMER), (2019), Published solar data, www.homerenergy.com/products/pro/docs/3.11 [Accessed March 3, 2021]
- [8] 7. Sogut O.S, & Durmayaz A. (2020), Performance optimization of a solar-driven heat engine with finite-rate heat transfer.
- [9] Rajput R.K. (2007), Engineering Thermodynamics (Third edition)
- [10] Duffie J.A., & Beckman W.A., (2013), Solar Engineering of Thermal Processes, Wiley and Sons, Chapter 3, Sections 3.1-3.10
- [11] Zhifeng Wang, (2019), Design of Solar Thermal Power Plants
- [12] Wijesundera N.E., & Hawlader M.N, (2021), Energy Developments: New Forms, Renewables, Conservation.
- [13] Kreetz M., Buck, R., & Krämer, K. (2018), Thermodynamic performance of a solar assisted micro gas turbine with central receiver. *Solar Energy*, 170, 311–324.
- [14] Zhang, H., Baeyens, J., Degreve, J., & Caceres, G. (2013). Concentrated solar power plants: Review and design methodology. *Renewable and Sustainable Energy Reviews*, 22, 466–481. <https://doi.org/10.1016/j.rser.2013.01.032>

- [15] Behar, O., Khellaf, A., & Mohammedi, K. (2015). A review of solar hybrid gas turbine systems. *Renewable and Sustainable Energy Reviews*, 39, 118–153. <https://doi.org/10.1016/j.rser.2014.07.014>
- [16] Koroneos, C., Spachos, T., & Moussiopoulos, N. (2003). Exergy analysis of renewable energy systems. *Energy*, 28, 295–310. [https://doi.org/10.1016/S0360-5442\(02\)00098-2](https://doi.org/10.1016/S0360-5442(02)00098-2)
- [17] Adeyemi, O. I., Ameen, O. M., & Abubakar, A. (2021). Techno economic assessment of solar gas hybrid power plants in Sub Saharan Africa. *Energy Reports*, 7, 1286–1298. <https://doi.org/10.1016/j.egy.2021.02.045>
- [18] Ramachandran J., & Conway M.C., (2022), GE Power Systems, Schenectady, NY, MS7001 – AN ADVANCED-TECHNOLOGY 70-MW CLASS 50/60... Hz GAS TURBINE
- [19] Nigerian Meteorological Agency. (2022). Meteorological data for Kaduna station (1991 – 2020). <https://www.nimet.gov.ng>